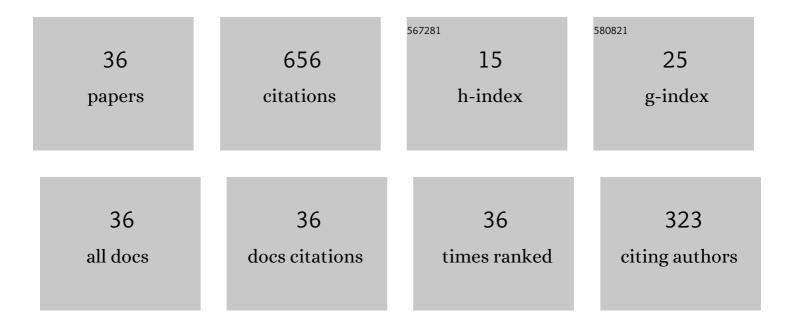
Jinlong Li

List of Publications by Year in descending order

Source: https://exaly.com/author-pdf/1142453/publications.pdf Version: 2024-02-01



#	Article	IF	CITATIONS
1	Constructing supramolecular self-assembled porous g-C3N4 nanosheets containing thiophene-groups for excellent photocatalytic performance under visible light. Applied Surface Science, 2022, 578, 152064.	6.1	58
2	A novel composite anode via immobilizing of Ce-doped PbO2 on CoTiO3 for efficiently electrocatalytic degradation of dye. Journal of Colloid and Interface Science, 2022, 608, 2921-2931.	9.4	30
3	Dual-emission ratiometric fluorescence probe based on copper nanoclusters for the detection of rutin and picric acid. Spectrochimica Acta - Part A: Molecular and Biomolecular Spectroscopy, 2022, 270, 120829.	3.9	18
4	Modification of hollow BiOCl/TiO2 nanotubes with phosphoric acid to enhance their photocatalytic performance. Korean Journal of Chemical Engineering, 2022, 39, 986-996.	2.7	11
5	Integration detection of mercury(<scp>ii</scp>) and GSH with a fluorescent "on-off-on―switch sensor based on nitrogen, sulfur co-doped carbon dots. RSC Advances, 2022, 12, 1989-1997.	3.6	16
6	Inverted design of oxygen vacancies modulated NiCo2O4 and Co3O4 microspheres with superior specific surface area as competitive bifunctional materials for supercapacitor and hydrogen evolution reaction. Journal of Energy Storage, 2022, 49, 104083.	8.1	22
7	ZIF-L-derived porous C-doped ZnO/CdS graded nanorods with Z-scheme heterojunctions for enhanced photocatalytic hydrogen evolution. International Journal of Hydrogen Energy, 2022, 47, 11190-11202.	7.1	52
8	Metal organic frameworks template-directed fabrication of rod-like hollow BiOClxBr1â^'x with adjustable band gap for excellent photocatalytic activity under visible light. Korean Journal of Chemical Engineering, 2022, 39, 2127-2137.	2.7	6
9	Maize starch derived boron doped carbon spheres via facile solvothermal route as the photoluminescence sensor for determination of pH and Cr(VI). Nanotechnology, 2022, 33, 275707.	2.6	2
10	Oxygen vacancies-rich NiCo2O4-4x nanowires assembled on porous carbon derived from cigarette ash: A competitive candidate for hydrogen evolution reaction and supercapacitor. Journal of Energy Storage, 2022, 50, 104280.	8.1	24
11	A facile selenic acid etching strategy for designing selenium-doped NiCo2O4/C nanoprisms with hollow/porous structure for advanced asymmetrical supercapacitor. Journal of Energy Storage, 2022, 50, 104714.	8.1	8
12	Oxygen vacancy rich and phosphate ions modulated hierarchical mesoporous NiCo2O4-CoO hollow nanocubes as efficient and stable electrodes for high-performance supercapacitor. Journal of Energy Storage, 2022, 52, 104849.	8.1	15
13	A novel self-activation strategy for designing oxygen vacancies-rich nickel ferrite and cobalt ferrite microspheres with large specific surface area for overall water splitting. International Journal of Hydrogen Energy, 2022, 47, 24343-24357.	7.1	12
14	Oxygen vacancy-engineered Fe2O3 porous microspheres with large specific surface area for hydrogen evolution reaction and lithium-sulfur battery. Colloids and Surfaces A: Physicochemical and Engineering Aspects, 2022, 649, 129476.	4.7	4
15	New excited state intramolecular proton transfer dyes based on naphthalenediimides (NDI) and its population of triplet excited state. Dyes and Pigments, 2021, 188, 109225.	3.7	1
16	Removal of volatile organic compounds from air using supported ionic liquid membrane containing ultraviolet-visible light-driven Nd-TiO2 nanoparticles. Journal of Molecular Structure, 2021, 1231, 130023.	3.6	26
17	Synthesis of bayberry-like hollow Gd/g-C3N4 nanospheres with high visible-light catalytic performance. Ionics, 2021, 27, 3185-3194.	2.4	7
18	A facile and novel dual-templating approach to discarded cigarette ash-derived high oxygen-containing porous carbon materials with nitrogen external defects for enhanced supercapacitors and hydrogen evolution reaction. Ionics, 2021, 27, 4013-4022.	2.4	3

JINLONG L

#	Article	IF	CITATIONS
19	Structure-designed synthesis of hollow/porous cobalt sulfide/phosphide based materials for optimizing supercapacitor storage properties and hydrogen evolution reaction. Journal of Colloid and Interface Science, 2021, 599, 577-585.	9.4	64
20	<i>In situ</i> fabrication of a Ni–Fe–S hollow hierarchical sphere: an efficient (pre)catalyst for OER and HER. New Journal of Chemistry, 2021, 45, 12996-13003.	2.8	18
21	Enhanced supercapacitive and hydrogen evolution reaction performance using hierarchically porous carbon derived from Viburnum Sargenti fruits. Ionics, 2021, 27, 1723-1731.	2.4	3
22	Hybrid-atom-doped NiMoO ₄ nanotubes for oxygen evolution reaction. New Journal of Chemistry, 2020, 44, 17477-17482.	2.8	17
23	lonic liquid promoted synthesis of nitrogen, phosphorus, and fluorine triple-doped mesoporous carbon as metal-free electrocatalyst for oxygen reduction reaction. lonics, 2020, 26, 4609-4619.	2.4	5
24	Preparation and characterization of g-C3N4/Ag–TiO2 ternary hollowsphere nanoheterojunction catalyst with high visible light photocatalytic performance. Journal of Alloys and Compounds, 2020, 823, 153851.	5.5	77
25	Synthesis of 3D flower-like structured Gd/TiO2@rGO nanocomposites via a hydrothermal method with enhanced visible-light photocatalytic activity. RSC Advances, 2019, 9, 31177-31185.	3.6	22
26	Preparation of a cerium/titanium composite with porous structure and enhanced visible light photocatalytic activity using β-cyclodextrin polymer microspheres as the template. Chemical Papers, 2018, 72, 369-379.	2.2	10
27	Synthesis and photocatalytic properties of visible-light-responsive, three-dimensional, flower-like La–TiO ₂ /g-C ₃ N ₄ heterojunction composites. RSC Advances, 2018, 8, 29645-29653.	3.6	23
28	Facile Synthesis and High Activity of Novel Composite C/Fe-BiVO4 Photocatalyst for Degradation of Cipfloxacin. Journal of Nanoscience and Nanotechnology, 2018, 18, 2472-2480.	0.9	1
29	Preparation of hollow Nd/TiO ₂ sub-microspheres with enhanced visible-light photocatalytic activity. RSC Advances, 2017, 7, 34857-34865.	3.6	23
30	CO ₂ separation from air using microporous polyvinylidene fluoride-supported triethylene glycol/alkanolamine liquid membranes. Materials Express, 2016, 6, 183-190.	0.5	3
31	Preparation and photocatalytic performance of a Pr–SiO ₂ –TiO ₂ nanocomposite for degradation of aqueous dye wastewater. Materials Express, 2016, 6, 1-9.	0.5	14
32	Photocatalytic Performance of a Nd–SiO ₂ –TiO ₂ Nanocomposite for Degradation of Rhodamine B Dye Wastewater. Journal of Nanoscience and Nanotechnology, 2015, 15, 1408-1415.	0.9	17
33	Photocatalytic Degradation of Dyestuff Wastewater with Zn ²⁺ –TiO ₂ –SiO ₂ Nanocomposite. Journal of Nanoscience and Nanotechnology, 2013, 13, 3972-3977.	0.9	2
34	Nanocomposite of Cu–TiO ₂ –SiO ₂ with High Photoactive Performance for Degradation of Rhodamine B Dye in Aqueous Wastewater. Journal of Nanoscience and Nanotechnology, 2012, 12, 6265-6270.	0.9	23
35	Air humidification by a liquid membrane of triethylene glycol. , 2011, , .		0
36	Separation of VOC vapor from air by a surface-soaked liquid membrane module using triethylene glycol. Separation and Purification Technology, 2009, 68, 283-287.	7.9	19